A&A 557, A113 (2013)
DOI: 10.1051/0004-6361/201321897

Astronomy & Astrophysics

Swift discovery of the orbital period of the high mass X-ray binary IGR J015712−7259 in the Small Magellanic Cloud *(Research Note)*

A. Segreto[1], G. Cusumano[1], V. La Parola[1], A. D'Aì[2], N. Masetti[3], and P. D'Avanzo[4]

[1] INAF – Istituto di Astrofisica Spaziale e Fisica Cosmica di Palermo, via U. La Malfa 153, 90146 Palermo, Italy
e-mail: cusumano@ifc.inaf.it
[2] Dipartimento di Fisica e Chimica, Università di Palermo, via Archirafi 36, 90123 Palermo, Italy
[3] INAF – Istituto di Astrofisica Spaziale e Fisica Cosmica di Bologna, via Gobetti 101, 40129 Bologna, Italy
[4] INAF – Brera Astronomical Observatory, via Bianchi 46, 23807 Merate (LC), Italy

Received 15 May 2013 / Accepted 13 August 2013

ABSTRACT

Context. In the past few years, the hard X-ray astronomy has made a significant step forward, thanks to the monitoring of the IBIS/ISGRI telescope onboard the INTEGRAL satellite and of the Burst Alert Telescope (BAT) onboard the *Swift* observatory. This has provided a huge amount of novel information on many classes of sources.
Aims. We have been exploiting the BAT survey data to study the variability and the spectral properties of the new high mass X-ray binary sources detected by INTEGRAL. We investigate the properties of IGR J015712−7259.
Methods. We performed timing analysis on the 88-month BAT survey data and on the XRT pointed observations of this source. We also report on the broad-band 0.2−150 keV spectral analysis.
Results. We find evidence of a modulation of the hard-X-ray emission with period P_o = 35.6 d. The significance of this modulation is 6.1 standard deviations. The broad band spectrum is modeled with an absorbed power law with photon index $\Gamma \sim 0.4$ and a steepening in the BAT energy range modeled with a cutoff at an energy of ∼13 keV.

Key words. X-rays: individuals: IGR J0157127259 – X-rays: binaries – binaries: close – stars: neutron

1. Introduction

Since the first years of the past decade, astronomy had two profitable protagonists in the hard X-ray energy band: the IBIS/ISGRI telescope (Ubertini et al. 2003; Lebrun et al. 2003) onboard the INTEGRAL satellite (Winkler et al. 2003) and the Burst Alert Telescope (BAT, Barthelmy et al. 2005) onboard of the *Swift* observatory (Gehrels et al. 2004). IBIS/ISGRI has conducted a fruitful exploration of the Galactic plane, revealing a large number of new X-ray sources: some of them are characterized by a strongly absorbed spectrum that made them elusive to previous soft X-ray monitoring; others show very bright transient episodes, and they were revealed thanks to the continuous scan of the Galactic plane. Many of these sources have been identified as high mass X-ray binaries (HMXBs), as inferred by the discovery of their optical counterparts (e.g., Filliatre & Chaty 2004; Reig et al. 2005; Masetti et al. 2006; Negueruela et al. 2006) or by the observation of long periodicities due to the occultation of the neutron star by the supergiant companion or to the enhancement of the neutron star accretion rate at periastron passage in an eccentric orbit. BAT is playing a momentous role in the study of many of these new INTEGRAL sources (e.g., Cusumano et al. 2010a; La Parola et al. 2010; D'Aì et al. 2011a,b). Thanks to a field of view two orders of magnitude larger than IBIS/ISGRI and to frequent changes in pointing direction, it efficiently records emission variability due to orbital eclipses or to the triggering of transient episodes.

IGR J015712−7259 is an X-ray binary that was discovered during the INTEGRAL scan of the Small Magellanic Cloud (SMC) and of the Magellanic Bridge in December 2008. A *Swift*-XRT follow-up observation found the soft X-ray counterpart at RA = 01h57m16.4s, Dec = −72°58′33″ (J2000) with an uncertainty localization of 3.8″ (90% confidence level, Coe et al. 2008), and the USNO (Monet et al. 2003) star USNO-B1 0170-0064697, which lies within the XRT error box, was associated with IGR J015712−7259. The *B* and *R* magnitudes of this star are 15.48 and 15.51, respectively (McBride et al. 2010). Timing analysis of the XRT and RXTE data has revealed a periodicity of ∼11.6 s (Coe et al. 2008). A broad band spectral analysis that combines the XRT and ISGRI data showed a flat power law spectrum ($\Gamma \sim 0.4$) with an exponential cutoff and a cutoff energy of ∼8 keV (McBride et al. 2010). This spectral shape is consistent with the spectrum typically shown by a HMXB.

This paper reports the results derived by the analysis of the soft and hard X-ray data collected by *Swift* on IGR J015712−7259, organized as follows. Section 2 describes the data reduction, and Sect. 3 reports on the timing analysis. In Sect. 4 we describe the spectral analysis, and in Sect. 5 we briefly discuss our results.

2. Observations and data reduction

We used the BATIMAGER code (developed for the analysis of coded mask telescopes data, see Segreto et al. 2010

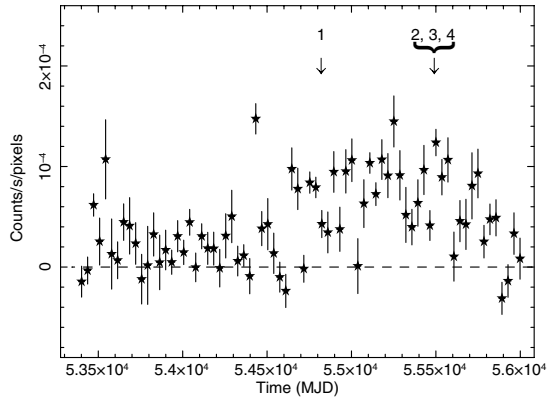

Fig. 1. IGR J015712−7259 BAT light curve the 15−45 keV energy range, with a bin length of 35 days. The epochs of the XRT observations are shown with vertical arrows.

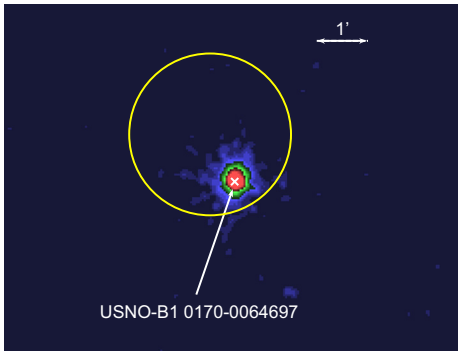

Fig. 2. 0.2−10 keV XRT image with superimposed the position of the optical counterpart, marked with a cross, and the BAT error circle of 1.61 arcmin (yellow circle).

for details) to analyze the data collected by *Swift*-BAT between November 2004 and March 2012 in survey mode. IGR J015712−7259 is detected in the 15−150 BAT all-sky map with a significance of ∼7 standard deviations in 88 months. The light curve of IGR J015712−7259 (Fig. 1) shows that the source was in a low intensity state in the first ∼33 months, rising to a higher state throughout the following months. The significance of the source in this second interval rises to ∼9 standard deviation in the 15−150 keV band, and it is maximized to ∼11 standard deviations in the 15−45 keV energy band. Therefore, to study the timing and spectral properties of the source, we used the BAT data collected after MJD 54 510. The light curve with the maximum resolution achievable with the BAT survey data was extracted in the 15−45 keV energy band.

The times were corrected to the solar system barycenter (SSB) using the task EARTH2SUN[1] and the JPL DE-200 ephemeris (Standish 1982). The background subtracted spectrum averaged over the entire survey period was extracted in eight energy channels and analyzed using the BAT redistribution matrix available in the *Swift* calibration database[2].

Swift-XRT observed IGR J015712−7259 four times, once in December 2008 (ObsID 00031313001) and three times in October 2010, for a total exposure time of ∼12 ks. The details of each XRT observation are in Table 1. All the observations are in photon counting mode (Hill et al. 2004).

[1] http://heasarc.gsfc.nasa.gov/ftools/fhelp/earth2sun.txt

[2] http://swift.gsfc.nasa.gov/docs/heasarc/caldb/swift/

Table 1. XRT observation log.

Obs #	Obs ID	T_{start} (MJD)	$T_{elapsed}$ (s)	Exposure (s)	Rate c/s	Phase
1	00031313001	54 820.3171	1985.7	1950.9	0.15	0.63
2	00041740001	55 474.6958	23 255.5	4613.9	0.02	0.03
3	00041740002	55 488.2508	4461.2	4443.4	0.16	0.41
4	00041740003	55 490.1957	29 626.6	4214.4	0.26	0.46

Notes. The quoted phase refers to the profile in Fig. 3c.

Data were processed with standard procedures, filtering and screening criteria (XRTPIPELINE v.0.12.4). Figure 1 shows the 0.2−10 keV XRT image where the soft X-ray counterpart of IGR J015712−7259 is well within the BAT error circle (1.61 arcmin). We extracted the source events from a circular region (20 pixel radius, with 1 pixel corresponding to 2.36 arcsec) centered on the source centroid, as calculated with XRTCENTROID (RA = 01h 57m 15.9s, Dec = −72°58′29.9″, error radius 3.6″). The source events' arrival times were corrected to the SSB using the task BARYCORR[3]. The background was extracted from an annular region with inner and outer radii of 40 and 70 pixels, respectively. XRT ancillary response files were generated with XRTMKARF[4]. The source and background spectra of each observation were averaged to obtain a single spectrum, and the ancillary files were combined using ADDARF, weighting them by the exposure times of the relevant spectra. Both the summed spectrum and each single spectrum were rebinned with a minimum of 20 counts per energy channel to allow the use of the χ^2 statistics. We used the spectral redistribution matrix v013. The spectral analysis was performed using XSPEC v.12.5. Errors are given at 90% confidence level, if not stated otherwise.

3. Timing analysis

The light curve of IGR J015712−7259 in the 15−45 keV energy range was investigated for the presence of periodic modulations. A timing folding analysis (Leahy et al. 1983) was applied to the baricentered arrival times. This method consists in building the light curve profile at different trial periods by folding the photon arrival times in N phase bins. For each trial profile, the χ^2 with respect to the average count rate is evaluated: a high χ^2 value will signal the presence of a periodic pulsation. We searched in the 0.5−500 d period range with a step resolution of $P^2/(N\,\Delta T)$, where P is the trial period, $N = 16$ is the number of folded profile phase bins, and ΔT (∼130 Ms) is the data time span. The average rate in each phase bin was calculated weighting the light curve rates by the inverse square of the relevant statistical error. This procedure, adopted to deal with the large span in statistical errors, is justified by the fact that the data are characterized by a wide range of signal-to-noise ratios because BAT monitors the source over a wide range of off-axis directions. Figure 3a shows the resulting periodogram. We find several features emerging over the χ^2 average trend. The feature at the lowest period is at $P_o = 35.6 \pm 0.5$ d ($\chi^2 \sim 132$) where the period and its error are evaluated as the position of the centroid and the standard deviation obtained from a Gaussian fit of the periodogram feature. The features at higher P turn out to be multiples of P_o.

The average χ^2 in the periodogram increases monotonically with the trial period deviating from what is expected for a white

[3] http://http://heasarc.gsfc.nasa.gov/ftools/caldb/help/barycorr.html

[4] http://heasarc.gsfc.nasa.gov/ftools/caldb/help/xrtmkarf.html

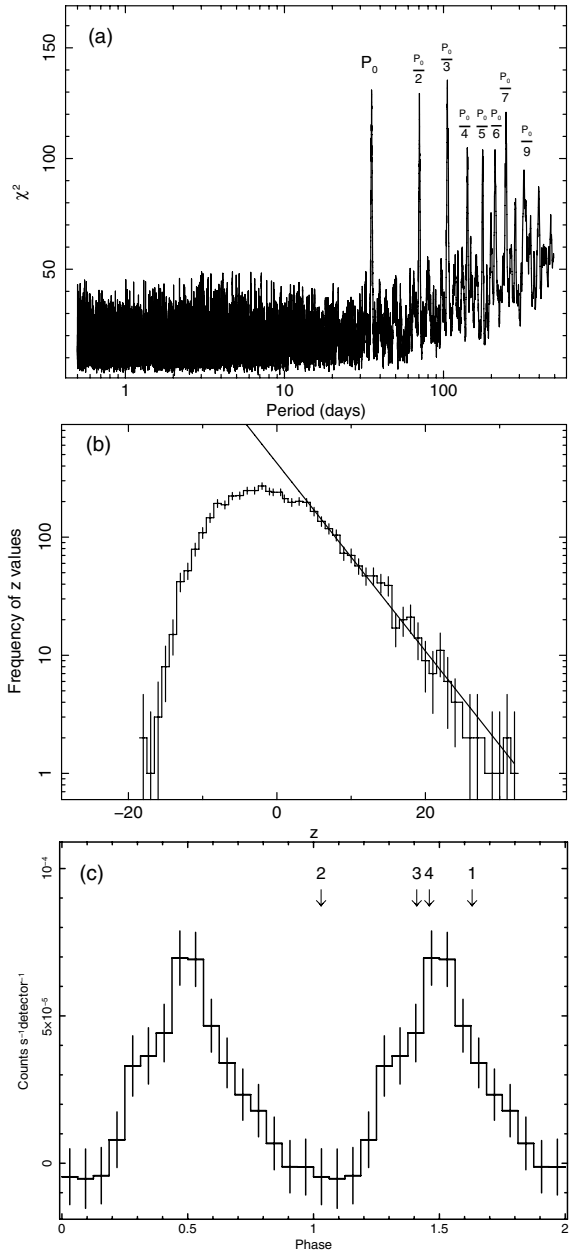

Fig. 3. **a)** Periodogram of *Swift*-BAT (15−45 keV) data for IGR J015712−7259. **b)** Histogram of the z ($\chi^2 - F_{\chi^2}$) distribution. The continuous line represents the best fit exponential model for $z > 20$. **c)** *Swift*-BAT light curve folded at a period $P_o = 35.6$ d, with 16 phase bins. Two orbital cycles are shown for clarity. The phase relevant to the epoch of each XRT observation is shown with a vertical arrow.

noise signal, where the χ^2 is expected to have an average value of $(N - 1)$. As a consequence, we cannot apply the χ^2 statistics to evaluate the significance of the feature at P_o, and an ad hoc procedure has to be used. The following steps summarize what we did to estimate the significance of the feature:

(1) We modeled the χ^2 distribution with a 2nd order polynomial to derive the average trend $F_{\chi^2}(P)$ of the χ^2 versus P.
(2) F_{χ^2} was then subtracted from the χ^2 distribution to obtain a flattened periodogram (hereafter, z). This allows the significance of the feature to be evaluated with respect to the average noise level of the periodogram. The value of z corresponding to P_o is ∼110.
(3) We built the histogram of the z distribution (Fig. 3b) from $P = 15$ d to $P = 55$ d (where the periodogram is characterized by a noise level that is quite consistent with the noise level at P_o) excluding the interval around P_o.
(4) We modeled the positive tail ($z > 5$) of the histogram with an exponential function.
(5) We evaluated the area (Σ) of the z histogram by summing the contribution of each single bin from its left boundary up to $z = 5$ and integrating the best-fit exponential function beyond $z = 5$ up to infinity.
(6) We evaluated the integral of the best-fit exponential function between $z = 110$ and infinity and normalized it by dividing by Σ.

The result (∼8.5×10^{-10}) is the probability of finding a z value ≥110 (or $\chi^2 \geq 132$), and it corresponds to a significance for the P_o feature of ∼6.1 standard deviations in Gaussian statistics.

In Fig. 3c we show the BAT light curve folded at P_o with $T_{epoch} = 55\,224.8086$ MJD. The profile is characterized by a single symmetric peak with a minimum consistent with zero intensity, whose centroid, evaluated by fitting the data around the dip with a Gaussian function, is at phase 1.01 ± 0.02, corresponding to MJD $(55\,225.2 \pm 0.7) \pm nP_o$. The peak is at phase 1.50 ± 0.02, corresponding to MJD $55\,242.6 \pm 0.7 \pm nP_o$.

The phase corresponding to the epochs of the XRT observations and referred to the folded BAT light curve are represented in Fig. 3c. The rates averaged over each observation (Col. 6 in Table 1) show variability in good agreement with the BAT rate profile.

To search for the pulsed modulation at ∼11.6 s, we applied the folding analysis to XRT pointings 1 and 4 in Table 1 (pointings 2 and 3 have low statistic content, with ∼70 counts each). The periodogram derived from observation 1 shows a feature at $P_s = 11.58 \pm 0.01$ s ($\chi^2 = 36.6$, 7 degrees of freedom [d.o.f.]), where the error is $P_s^2/(N\Delta T)$, with $N = 8$, confirming the result reported by Coe et al. (2008). The probability of a chance occurrence for a feature with such a χ^2 value at 11.6 s is $\sim 8 \times 10^{-6}$, corresponding to a significance of ∼4.5 standard deviations in Gaussian statistics. The periodogram of observation 4 does not show any significant feature. We also performed a folding analysis on each of the five snapshots of observation 4, without finding any significant feature either in each single snapshot periodogram or in the periodogram produced by their sum.

4. Spectral analysis and results

The broad band spectral analysis puts together XRT data of different epochs and BAT data accumulated over the 88-months of monitoring. We therefore performed a preliminary analysis to verify that no significant spectral variability affects the four XRT observations and during the BAT monitoring. The background subtracted spectra of each single XRT observation were fitted simultaneously with an absorbed power law with the photon index and absorbing column density forced to have the same value for the four datasets. This model, yielding a best fit photon index of 0.99 ± 0.12 and N_H of $(1.5 \pm 0.5) \times 10^{21}$ cm^{-2}, produced residuals with a similar trend for all the datasets. Different BAT spectra were also produced by selecting the data in different time intervals (MJD intervals 53 383.478−54 593.061, 54 593.061−55 233.428, and 55 233.428−56 016.101; see Fig. 1) and in three different phase intervals ([0.94−1.31], [0.31−0.44, 0.69−0.81], and [0.44−0.69], see Fig. 3). These spectra were fitted with a power law model and, as above, we forced the photon

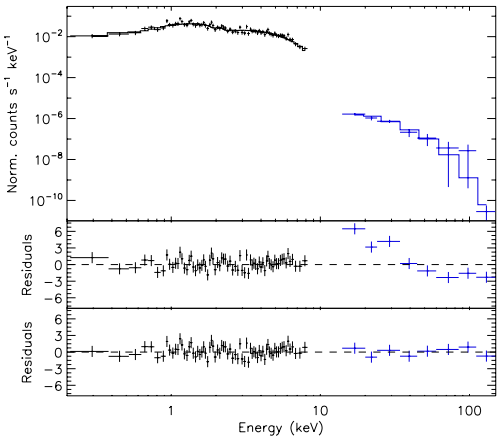

Fig. 4. IGR J015712−7259 broad band spectrum. *Top panel*: XRT and BAT data and best fit `phabs*cutoffpl` model. *Central panel*: residuals in unit of standard deviations for the `phabs*powerlaw` model. *Bottom panel*: residuals in unit of standard deviations for the `phabs*cutoffpl` model.

Table 2. Best fit spectral parameters.

Parameter	Cutoff pl	Units
$N_{\rm H}$	$<5\times10^{20}$	cm^{-2}
Γ	$0.4^{+0.1}_{-0.1}$	
$E_{\rm cut}$	$13^{+4.0}_{-3}$	keV
N	$5.2^{+0.6}_{-0.4}\times10^{-4}$	ph/(keV cm^2 s) at 1 keV
$C_{\rm BAT}$	$0.4^{+0.2}_{-0.1}$	
F (0.2−10 keV)	$1.26^{+0.11}_{-0.12}\times10^{-11}$	erg cm^{-2} s^{-1}
F (15−150 keV)	$9.1^{+1.5}_{-2.4}\times10^{-12}$	erg cm^{-2} s^{-1}
χ^2	70.1 (75 d.o.f.)	

Notes. $C_{\rm BAT}$ is the constant factor to be multiplied by the model in the BAT energy range in order to match the BAT data. We report unabsorbed fluxes for the characteristic XRT (0.2−10 keV) and BAT (10−150 keV) energy bands.

index to assume the same value for all the spectra, thereby leaving the normalization free to vary. The residuals between best fit model and data showed a similar trend for all the datasets. The best fit photon index is 2.0 ± 0.2.

The broad band spectral analysis was then performed by coupling the 15−150 keV BAT spectrum extracted from the data collected after MJD 54 510 and the XRT spectrum obtained by adding the individual XRT spectra (see Sect. 2). A multiplicative factor that disengages the normalization parameter of the model for the two datasets was introduced in the fit to take both the intercalibration uncertainty between XRT and BAT and the non simultaneity of the data into account. We started fitting the data with an absorbed power law model `phabs*(powerlaw)`. This model yields an unacceptable $\chi^2 = 149.7$, with 76 dof and is not able to describe the BAT data, as shown in Fig. 4, (middle panel). The steepening in the BAT energy range (see Fig. 4) suggests the presence of a cutoff. Indeed, the spectrum turned out to be described much better when adopting the model `phabs*cutoffpl` (see Table 2) with a photon index Γ of ∼0.4 and a folding energy of ∼13 keV, resulting in a $\chi^2 = 70.1$, for 75 d.o.f. The hydrogen column density is lower than 5×10^{20} cm^{-2}. Figure 4 shows data and best fit model (top panel) and residuals (bottom panel) for the cutoff power law model.

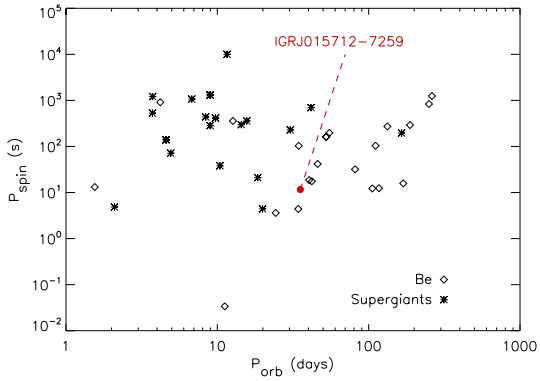

Fig. 5. The Corbet diagram plots the spin period versus the orbital period for HMXBs. Diamond and star points represent the Be and supergiant systems, respectively. The red filled circle marks the position of IGR J015712−7259.

5. Conclusions

IGR J015712−7259, discovered by INTEGRAL in the SMC, is a HXMB with an X-ray emission modulated by a spin period of 11.6 s (Coe et al. 2008). The timing analysis of the BAT survey data has allowed a new piece of information on this binary system to be added, with the discovery of a long term periodic modulation in its hard X-ray emission at $P_{\rm o} = 35.6$ d. The significance of this result is ∼6.1 standard deviations in Gaussian statistics. We interpret this modulation as the orbital period of the binary system. Knowing it and the spin period allows us to locate the source on the Corbet diagram (Corbet 1986), where its position is consistent with the Be X-ray binaries' region (Fig. 5). On the other hand, the BAT light curve folded at $P_{\rm o}$ shows a triangular symmetric peak with a minimum consistent with zero intensity suggesting that accretion happens for most of the orbit. The minimum could be related to the occultation of the neutron star by the companion star. This behavior is not typical of HXRB with a Be companion, which are usually observed through short-lived enhancements of their emission caused by accretion episodes driven by disk instabilities and by the periastron passage in a highly eccentric orbit.

The BAT long-term light curve (Fig. 1) shows that this source has enhanced its hard X-ray activity since early 2009, after showing a modest intensity level in the first three years of the survey monitoring. This behavior prevented the source from being reported in the first Palermo BAT catalogs (Cusumano et al. 2010b,c), while it is listed with a significance of ∼10 standard deviations in the latest issue of the catalog[5] (which covers 66 months of survey). The INTEGRAL detection reported by Coe et al. (2008) is located in time during the early stages of enhanced emission.

The broad-band (0.2−150 keV) spectral analysis of IGR J015712−7259 was performed by combining all the available *Swift*-XRT observations and the BAT spectrum extracted from the data collected after MJD 54 510 when the source is observed to be in a high-intensity state. The data are described well by a flat ($\Gamma \simeq 0.4$) power law with a cut-off at ∼13 keV. This spectral shape is commonly observed among HMXBs. The best fit parameters agree with the analysis reported by McBride et al. (2010) based on the 2008 December XRT observation and on the ISGRI data.

The results reported above need to be integrated with optical observations aimed at identifying the spectral type of the

[5] http://bat.ifc.inaf.it

companion star. This will allow the class of this binary system to be ascertained and more constraints to be set on its orbital characteristics.

Acknowledgements. This work has been supported by ASI grant I/011/07/0.

References

Barthelmy, S. D., Barbier, L. M., Cummings, J. R., et al. 2005, Space Sci. Rev., 120, 143
Coe, M. J., McBride, V. A., Bird, A. J., et al. 2008, ATEL 1882
Corbet, R. H. D. 1986, MNRAS, 220, 1047
Cusumano, G., La Parola, V., Romano, P., et al. 2010a, MNRAS, 406, L16
Cusumano, G., La Parola, V., Segreto, A., et al. 2010b, A&A, 524, A64
Cusumano, G., La Parola, V., Segreto, A., et al. 2010c, A&A, 510, A48
D'Aì, A., Cusumano, G.,La Parola, V., et al. 2011a, A&A, 532, A73
D'Aì, A., La Parola, V., Cusumano, G., et al. 2011b, A&A, 529, A30
Filliatre, P., & Chaty, S. 2004, ApJ, 616, 469
Gehrels, N., Chincarini, G., Giommi, P., et al. 2004, ApJ, 611, 1005
Hill, J. E., Burrows, D. N., Nousek, J. A., et al. 2004, Proc. SPIE, 5165, 217
La Parola, V., Cusumano, G., Romano, P., et al. 2010, MNRAS, 405, L66
Lebrun, F., Leray, J. P., Lavocat, P., et al. 2003, A&A, 411, L141
Leahy, D. A., Darbro, W., Elsner, R. F., et al. 1983, ApJ, 266, 160
Masetti, N., Morelli, L., Palazzi, E., et al. 2006, A&A, 459, 21
McBride, V. A., Bird, A. J., Coe, M. J., et al. 2010, MNRAS, 403, 709
Monet, D. G., Levine, S. E., Canzian, B., et al. 2003, AJ, 125, 984
Negueruela, I., Smith, D. M., Reig, P., Chaty, S., & Torrejón, J. M. 2006, The X-ray Universe 2005, ed. A. Wilson, ESA SP, 604, 165
Reig, P., Negueruela, I., Papamastorakis, G., Manousakis, A., & Kougentakis, T. 2005, A&A, 440, 637
Segreto, A., Cusumano, G., Ferrigno, C., et al. 2010, A&A, 510, A47
Standish, E. M., Jr. 1982, A&A, 114, 297
Ubertini, P., Lebrun, F., Di Cocco, G., et al. 2003, A&A, 411, L131
Winkler, C., Courvoisier, T. J.-L., Di Cocco, G., et al. 2003, A&A, 411, L1